

# Method for Isolation and Detection of Ketones Formed from High-Temperature Naphthenic Acid Corrosion

Logan C. Krajewski,<sup>†</sup> Vladislav V. Lobodin,<sup>‡</sup> Winston K. Robbins,<sup>§</sup> Peng Jin,<sup>||</sup> Gheorghe Bota,<sup>||</sup> Alan G. Marshall,<sup>\*,†,‡</sup> and Ryan P. Rodgers<sup>†,‡</sup>

<sup>†</sup>Department of Chemistry and Biochemistry, Florida State University, 95 Chieftain Way, Tallahassee, Florida 32306, United States

<sup>‡</sup>Ion Cyclotron Resonance Program, National High Magnetic Field Laboratory, and <sup>§</sup>Consultant, Future Fuels Institute, Florida State University, 1800 East Paul Dirac Drive, Tallahassee, Florida 32310, United States

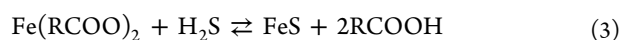
<sup>||</sup>Institute for Corrosion and Multiphase Technology, Ohio University, 342 West State Street, Athens, Ohio 45701, United States

## Supporting Information

**ABSTRACT:** Corrosion control at refineries remains a challenge because the mechanism of naphthenic acid (NAP) corrosion is still not fully understood. The rate of NAP corrosion does not correlate with acidity (as measured by total acid number); therefore, it has been suggested that a subset of NAP in petroleum fractions may be more corrosive than others. Because the primary corrosion product (iron naphthenates) may thermally decompose to ketones at corrosion temperatures (250–400 °C), ketones in corrosion fluids could potentially be used to implicate specific problematic acids in corrosion tests. To that end, we have developed a method for isolating and characterizing ketones in corrosion test solutions. Ketones from tests on palmitic and 4-cyclohexyl pentanoic acids (C<sub>16</sub>H<sub>32</sub>O<sub>2</sub> and C<sub>11</sub>H<sub>20</sub>O<sub>2</sub>) have been successfully isolated with a strong anion exchange solid-phase separation. Gas chromatography/mass spectrometry identifies ketones formed as a result of model acid corrosion. Fourier transform ion cyclotron resonance mass spectrometry further confirms the detection of these ketones and structurally confirms ketones by use of a commercially available reagent that targets ketones and aldehydes. Additional oxygen species generated in the corrosion test likely result from reactions between dissolved atmospheric oxygen and the mineral oil matrix. With this method now validated, it can be applied in future studies of more complex acid mixtures to determine any structural specificity in naphthenic acid corrosion.

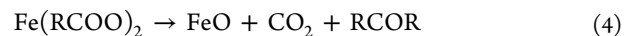
## 1. INTRODUCTION

Corrosion is a major concern of the petroleum industry, with over \$26 billion spent annually on corrosion issues.<sup>1</sup> To fulfill worldwide energy demand, oil companies are turning increasingly toward “opportunity crudes” that are sold at discounted prices due to the presence of naphthenic acids (NAP), the natural carboxylic acids found in petroleum. NAP concentration in petroleum is commonly measured by total acid number (TAN, the amount of potassium hydroxide in milligrams needed to neutralize one gram of oil). The NAP can cause severe corrosion in refinery distillation between 240 and 400 °C. This problem has resulted in an increased interest in NAP corrosion and its mechanism.<sup>2–5</sup> Under refinery conditions, NAP corrosion is accompanied by reactive sulfur corrosion, generally represented by the reactions seen in eqs 1–3:<sup>6</sup>



Although iron naphthenate is commonly considered to be oil-soluble, the corrosion product, iron sulfide (FeS), is not. Thus, corrosion is accompanied by the formation of a scale that is somewhat protective by acting as permeation barrier that inhibits further corrosion, making correlations with TAN difficult.<sup>6</sup>

To date, no strong correlation has been demonstrated between TAN and corrosion, as measured by mass of iron lost from coupons under test conditions, other than that corrosion generally increases with increased acid concentration.<sup>7</sup> The lack of correlation is often attributed to differences in structural shape or molecular weight of NAP from different sources or to interactions between NAP and sulfidation corrosion.<sup>6,8–13</sup> Measuring yields of hydrogen gas formed from eq 1 or the amount of soluble iron (iron naphthenates also formed in eq 1) has been inconclusive in correlations with TAN.<sup>14</sup> In the latter experiments, carbon dioxide (CO<sub>2</sub>) has been detected in the gas phase above a threshold temperature of 250 °C.<sup>14</sup> Because CO<sub>2</sub> is not generated as a result of NAP or reactive sulfur corrosion (eqs 1–3), it was proposed that it was formed as a result of the thermal decomposition of iron carboxylates to ketones and insoluble iron oxide:<sup>15,16</sup>



in which alpha iron denotes ferrite. Thermal decomposition of iron carboxylates begins at 250 °C, below the threshold temperature for thermal degradation of NAP (~350 °C).<sup>14,17</sup> Because FeO is not stable, it disproportionates to magnetite

Received: June 23, 2017

Revised: August 25, 2017

Published: September 13, 2017

(Fe<sub>3</sub>O<sub>4</sub>) and ferrite (eq 5).<sup>18,19</sup> A protective inner layer containing magnetite has been detected underneath the FeS scale,<sup>20,21</sup> spurring renewed interest in these secondary iron carboxylate reactions, with patents issued to analyze either ketones or magnetite as a means to develop a correlation between TAN and corrosion.<sup>22,23</sup>

The ketones formed by iron naphthenate decomposition in corrosion offer an opportunity to gain insight into the specific NAP responsible for corrosion because the ketone's structure is related to the acids that reacted to form the iron naphthenate. As noted above, it has been proposed that NAP molecular structure and especially NAP molecular weight affect the corrosivity of the acids. Specifically, it has been hypothesized that lower molecular weight NAP are more corrosive than their higher molecular weight (MW) counterparts. Previous studies have unsuccessfully attempted to isolate and characterize the iron salts by selective ion exchange separations.<sup>24</sup> Here, we consider the possibility of distinguishing corrosive acids by characterizing the ketones formed by thermal decomposition of the iron naphthenates. Because it has been demonstrated that NAP in crude oils include tens of thousands of individual compounds with MW between 200 and 1000 Da,<sup>25,26</sup> the ketones that might be formed by eq 4 could range from carbon numbers C<sub>20</sub> to C<sub>100</sub>. Furthermore, metal oxides, such as the magnetite formed during corrosion, may act as a catalyst that promotes ketonic decarboxylation without direct involvement of iron.<sup>27,28</sup> Thus, a method that has the potential for characterizing acids is needed for identification of ketones formed during corrosion tests or by catalytic decarboxylation products of petroleum oils. Results obtained with this method can contribute to corrosion models for refinery corrosion control. Such a method needs to cover this wide MW range that exceeds the capabilities of gas chromatography (GC). Here, we report the initial stages of the development of a method for characterizing NAP ketone products, based on chromatographic separation and Fourier transform ion cyclotron resonance mass spectrometry (FT-ICR MS) identification.

The characterization of moderately polar ketones in corrosion test fluids requires their prior separation from higher concentrations of nonpolar hydrocarbons, moderately polar iron naphthenates, and polar NAP hydrocarbons. The requisite method is based upon ketones generated in a laboratory high-temperature corrosion test with mineral oil spiked with two model acids: palmitic acid (PA), which serves as a simple model acid, and 4-cyclohexyl pentanoic acid (CxPA), which is comparable in size and structure to the lower MW NAP found in petroleum.<sup>29,30</sup> Here, the separation of these relatively simple low-MW ketones can be monitored by both GC and MS techniques. However, as highlighted earlier, application to real-world samples will increasingly depend on FT-ICR MS.

## 2. EXPERIMENTAL METHODS

**Corrosion Test Samples.** A white mineral oil, with an average molecular weight of 530 Da, was spiked with either palmitic acid (C<sub>16</sub>H<sub>32</sub>O<sub>2</sub>, 256.4 Da) or 5-cyclohexyl pentanoic acid (CxPA, C<sub>11</sub>H<sub>20</sub>O<sub>2</sub>, 184.3 Da) to give the solution a TAN of 1.75. The samples were pretreated in an autoclave as previously described in a high-temperature corrosion test.<sup>15,16</sup> Briefly, three A-106 carbon steel and three A335-P9 (9 Cr Alloy) rings, with a total surface area of ~300 cm<sup>2</sup>, were pretreated with 600 g of model acid solution. The rings were placed in a stirred autoclave in which model acid solution was added and the autoclave sealed. The autoclave headspace was flushed with nitrogen for 5 min, pressurized with nitrogen to 100 psi, and the temperature raised to and maintained at 316 °C for 24 h. At the end of

the test, the oil samples in the autoclave were collected for analysis. In addition to the two model acid solutions, the corrosion test was performed for a white mineral oil blank.

**Ketone Separation.** The ketones in the oil samples were isolated based on the separation scheme outlined in Figure 1. A strong anion

<b>SAX Extraction</b>		<b>Palmitic Acid</b>	<b>4-Cyclohexyl pentanoic acid (CxPA)</b>
Conditioned with DCM, pentane		<b>Mass Recovery</b>	<b>Mass Recovery</b>
<b>Pentane</b>	100%, 12 mL	94.0 %	94.0 %
<b>DCM</b>	100%, 12 mL	3.4 %	2.7 %
<b>Methanol</b>	100%, 12 mL	1.1 %	0.5 %
<b>Total Mass Recovery:</b>		<b>98.5 %</b>	<b>97.2 %</b>

**Figure 1.** Strong anion exchange (SAX) separation scheme and mass recovery. Most recovered mass is found in the pentane fraction and represents hydrocarbons. Acids are eluted in the methanol fraction, with transformed acid products found in the DCM fraction. Approximately all mass from the blank (white mineral oil) sample is recovered in pentane fraction (~98.0%, not shown).

exchange (SAX) solid phase extraction cartridge (Agilent Bond Mega BE-SAX) (SPE) containing 2 g of sorbent was preconditioned with 12 mL of 100% dichloromethane (DCM) followed by 12 mL of 100% pentane prior to use. Aliquots (~1 g) of sample (post-test model acid) solution diluted in 2 mL of pentane were loaded onto and allowed to equilibrate on the column for ~10 min. Fractions were then collected through 12 mL successive washes with pentane, DCM, and methanol (MeOH). All fractions were stripped of solvent under a gentle stream of nitrogen and then dissolved to 1 mg/mL in toluene to form a stock solution for further use. All solvents were HPLC grade from J.T. Baker chemicals (Phillipsburg, PA) and used as received. This separation takes advantage of interactions between the quaternary amine group of the stationary phase and the polar species in the solutions. We hypothesized that the bulk of each sample is nonpolar hydrocarbons from the mineral oil that would have no interaction with the stationary phase, so that they elute with pentane. Ketones are moderately polar and are eluted in the second fraction with DCM. Acids are more strongly retained on the basic surface of the stationary phase but are partially eluted with methanol.<sup>31,32</sup> The acid retention mechanism is likely not ion exchange because the interactions occur under nonaqueous conditions for which protonation and deprotonation are unlikely.

**GC-MS Analysis.** Liquid chromatography SAX fractions were analyzed by GC-MS with an Agilent 5973 mass spectrometer equipped with an HP 6890 gas chromatograph. One microliter of sample was injected into the GC inlet (280 °C) with a 1:10 split ratio. An Agilent DB-5MS fused silica capillary column (30 m long, 0.25 mm inner diameter, and 0.25 μm film thickness) was used for separation with helium (99.9997% purity) carrier gas at 1.2 mL min<sup>-1</sup>. The oven temperature was programmed from 50 °C for 3 min and then ramped at 10 °C min<sup>-1</sup> to a final temperature of 300 °C, at which it was held for 15 min. The transfer line was kept at 300 °C. The ion source was held at 200 °C. Electron ionization (EI) mass spectra were acquired in the *m/z* range of 30–650 at a rate of 1 scan s<sup>-1</sup>. Total ion current (TIC) was used to reconstruct the chromatographic signal.

**Ketone Derivatization.** FT-ICR analysis provides accurate molecular weights, which in turn provide the elemental composition for nearly all of the peaks in the mass spectrum. However, elemental composition alone does not provide structural and/or chemical functionality information required for ketone identification. Therefore,

the ketone fraction isolated by the liquid chromatography SAX method was subsequently derivatized with Amplifex keto reagent (AB Sciex, Framingham, MA) as described elsewhere<sup>33</sup> to confirm the GC-MS results by FT-ICR MS. Sample solution (200  $\mu$ L) was added to 200  $\mu$ L of the derivatization reagent. The sample-reagent solution was mixed for 1 h at room temperature with mechanical agitation and dried with a gentle flow of nitrogen gas.

**Sample Preparation for FT-ICR MS Analysis.** The stock liquid chromatography fractions (1 mg/mL) were diluted to 500  $\mu$ g/mL with methanol. High-purity formic acid (MS grade, Sigma-Aldrich, St. Louis, MO) was added as a modifier to a final concentration of 5% (v/v). High formic acid content was chosen because previous studies have shown that it aids in the protonation of ketones.<sup>34</sup> Derivatized fractions were diluted to 500  $\mu$ g/mL in toluene:methanol (50:50, v/v). Because the derivatized ketones contain a quaternary ammonium group, they are efficiently ionized by (+) ESI without a need for additional modifier. A syringe pump, with a flow rate of 500 nL/min, was used to deliver the samples through the 50  $\mu$ m inner diameter fused silica micro ESI needle. The samples were delivered under typical ESI conditions (i.e., 3.0 kV with a heated metal capillary temperature of  $\sim$ 100  $^{\circ}$ C).

**Mass Analysis.** Samples were analyzed with a custom-built passively shielded 9.4T FT-ICR mass spectrometer,<sup>35</sup> equipped with a modular software package for data acquisition (Predator).<sup>34,36</sup> Positive ions were generated at atmospheric pressure and transferred into the mass spectrometer by a tube lens/skimmer at 350 V for the whole fractions and 250 V for the derivatized samples. Ions were accumulated in an rf-only external quadrupole,<sup>37</sup> passed through a mass resolving rf-only quadrupole, collisionally cooled with helium gas ( $\sim$ 3.5  $\times$  10<sup>-6</sup> Torr) before transfer by octopole ion guides with capacitively coupled excitation electrodes into a seven-segment cylindrical cell.<sup>38,39</sup> A broadband frequency-sweep ("chirp") excitation ( $\sim$ 70–720 kHz at a sweep rate of 50 Hz/ $\mu$ s and peak-to-peak amplitude,  $V_{p-p}$ , of 0.57 V) was used for detection. For each sample, 150 time domain transients were coadded,<sup>40</sup> zero-filled, fast Fourier transformed, and phase-corrected to yield an absorption-mode mass spectrum.<sup>41</sup>

**Mass Calibration and Data Analysis.** Mass spectra were externally calibrated with HP mix (Agilent, Santa Clara, CA), and ICR frequencies were converted to  $m/z$  based on quadrupole trapping potential approximation.<sup>42,43</sup> Peak lists were constructed from peaks of magnitude at least six times greater than the standard deviation of the baseline noise. The spectra were then internally calibrated by use of a "walking" calibration<sup>40</sup> based on the most abundant homologous ion series. Ion masses were converted to the Kendrick mass scale, assigned an elemental composition, and grouped by heteroatom class ( $O_nN_nS_n$ ) differing in the extent of alkylation (e.g.,  $O_2$  class contains all species with two oxygens in addition to the hydrocarbon backbone).<sup>44</sup> Custom software (PetroOrg©) was used for data calibration, elemental composition assignment, and imaging.<sup>45</sup> Peak assignments were limited to elemental compositions containing less than 100 <sup>12</sup>C, 200 <sup>1</sup>H, 2 <sup>14</sup>N, 5 <sup>16</sup>O, and 1 <sup>32</sup>S atoms. All assigned heteroatom classes with a relative abundance greater than 1% were visualized.

### 3. RESULTS AND DISCUSSION

**Isolation of Ketones.** The long-term goal of this work is to use ketones produced by NAP corrosion in heavy vacuum gas oils (HVGO) to identify differences in naphthenic acid reactivity. Because not all of the acids in an HVGO react during a corrosion test, we sought conditions to adequately separate ketones from hydrocarbons and residual acids to facilitate identification by MS. Due to the high level of HVGO naphthenic acid compositional complexity, we first developed the method with solutions from corrosion tests for model acids in a mineral oil matrix. Previously, NAP acids have been successfully separated from HVGO with aminopropyl silica (APS) SPE cartridges.<sup>46,47</sup> Here, an SAX SPE cartridge was

chosen to avoid the possible formation of Schiff bases by reaction of the ketone with the free amine on APS. Although the SAX sorbent has been used for acid isolation, it generally requires the addition of a low-MW acid (i.e., formic or acetic) in an alcohol solvent for complete acid recovery.<sup>31,32</sup> Most (94.0%) of the recovered mass, determined gravimetrically, for both test samples (PA and CxPA) resides in the pentane fraction (Figure 1), as expected, because the samples consist primarily of mineral oil composed of paraffinic and naphthenic hydrocarbons. The DCM fractions, expected to contain the ketones, make up 3.4% and 2.7% of the PA and CxPA samples. The subsequent MeOH fractions comprise 1.1% and 0.5% of the recovered mass. As discussed below, these more polar species are likely to include some acid "bleed" from the cartridge and byproducts of oxidation of the mineral oil during the corrosion test. The 1.5% and 2.8% of mass not recovered for the PA and CxPA samples likely arise from incomplete recovery of unreacted acid and/or any highly polar species from mineral oil oxidation. Nearly all of the mass recovered from the test for the mineral oil blank ( $\sim$ 98.0%), was in the pentane fraction, whereas the DCM and MeOH fractions each have negligible mass (<0.1%).

**Confirmation by GC-MS.** Because the corrosion tests were run with single low-MW model acids, the fractions isolated from the samples are of low compositional complexity and were therefore analyzed by GC-MS to validate efficient separation of species. The TIC for each of the three fractions derived from the palmitic acid sample is shown in Figure 2. The pentane

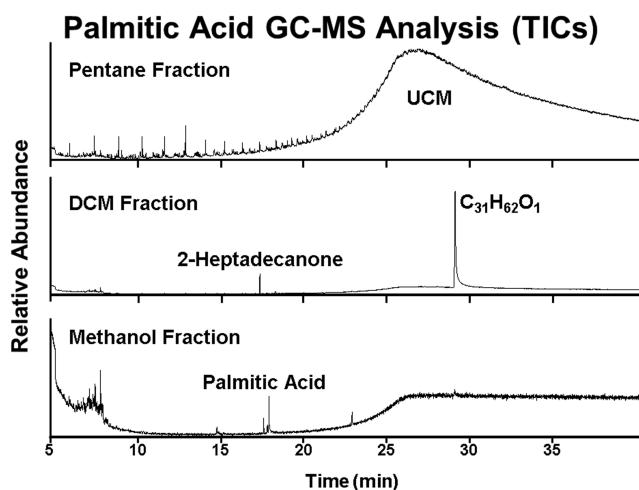


**Figure 2.** Total ion chromatogram (TIC) for the SAX fractions from the palmitic acid sample. The pentane fraction is composed of an unresolved complex mixture (UCM) of hydrocarbons. The DCM fraction is composed of two peaks, library-identified as the indicated ketones. Residual palmitic acid is seen in the methanol fraction.

fraction is dominated by an unresolved complex mixture (UCM) that starts from a retention time of approximately 15 min to the end of the chromatographic run. This nonpolar UCM is consistent with the complex mixture of hydrocarbons in the mineral oil used in the corrosion test. The DCM fraction is dominated by a large peak with a retention time of  $\sim$ 27 min. This peak is identified by an EI MS fragmentation library database search as a  $C_{31}H_{62}O_1$  ketone, which corresponds to the ketone that would form from the decomposition of iron(II) palmitate. A much smaller peak with a retention time of  $\sim$ 17 min was identified in similar manner as 2-heptadecanone. We

hypothesize that this molecule may be formed from the cracking of  $C_{31}H_{62}O_1$  between the alpha and beta carbon of the carbonyl during the corrosion test. As previously documented, long-chain fatty acid esters are known to thermally decompose by such a mechanism at temperatures below those used in the corrosion test.<sup>48,49</sup> A small UCM is visible starting with a retention time of  $\sim 23$  min, believed to result from species formed from dissolved oxygen (discussed below) that was not removed from the sample prior to the corrosion test. The small peak at  $\sim 18$  min in the TIC for the MeOH fraction is assigned to residual unreacted palmitic acid. Any UCM in this fraction, as for the DCM fraction, presumably results from species that reacted with dissolved oxygen. The TIC for the CxPA sample fractions demonstrated similar results (see Supporting Information Figure S-1). However, only a single peak was observed for the DCM fraction, suggesting that the nonlinear ketone is less prone to thermal fragmentation. The GC-MS for blank fractions did not contain any resolved peaks.

**FT-ICR-MS Analysis.** GC-MS analysis of model acid corrosion test solutions confirms a clean separation of model ketones (formed in corrosion tests) from the hydrocarbon matrix and any residual acids. However, ketones produced in future corrosion tests of higher molecular weight HVGO acids are anticipated to have too high boiling point and be too compositionally complex for GC-MS speciation. Consequently, we applied FT-ICR MS (which provides access to high-MW species) to detect and identify isolated ketones. As expected, the first (pentane) fraction contains only nonpolar hydrocarbons, which do not ionize under (+) ESI conditions; therefore, no peaks were detected in those fractions by FT-ICR. The ions detected in the second (ketone) chromatographic fraction were assigned molecular formulas based on mass, grouped together in a single class based on heteroatom content and the relative abundances of the various heteroatom classes compared (Figure 3). In all three samples, the  $O_1$  class, which would contain compounds that contain only one carbonyl group and no additional oxygen, is the most abundant. Model mixtures of PA and CxPA, however, have a significantly higher  $O_1$  class abundance than the blank, suggesting an enrichment of

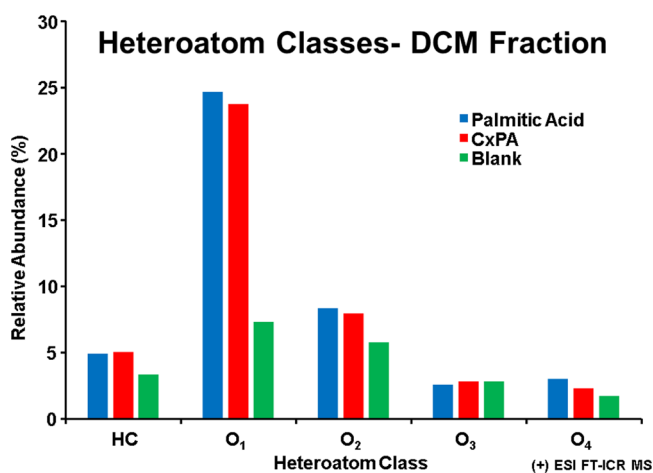


**Figure 3.** Distribution of heteroatom classes with relative abundance higher than 1%, from the DCM fraction of the SAX separation. The palmitic acid and CxPA samples are dominated by the  $O_1$  class, whereas other classes exhibit relative abundance similar to those for the blank sample. Data were derived from (+) ESI 9.4 T FT-ICR mass spectra.

that class as a result of species formed from the acids spiked into the mineral oil. Although additional classes (hydrocarbons (HC),  $O_2$ , and  $O_3$ ) are detected, the abundances of all of those classes are similar for all three samples, suggesting partial oxidation of the mineral oil during the corrosion test.

Isoabundance-contoured plots of double bond equivalents (DBE = number of rings plus double bonds to carbon) versus number of carbon atoms serve to visualize the compositional distribution for members of the assigned  $O_1$  class in the ketone fraction (Figure 4). The plots for PA and CxPA each exhibit

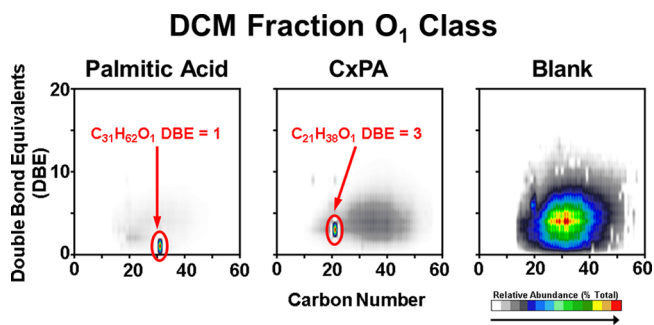


**Figure 4.** Double bond equivalents (DBE) versus carbon number plots for members of the  $O_1$  class. The palmitic and CxPA acid samples are dominated by a single peak, assigned the indicated molecular formula. Additional assigned species are seen at lower abundance and in the sample blank and are believed to result from reactions with dissolved oxygen and the mineral oil during the high-temperature corrosion test.

one high-magnitude peak, of assigned elemental composition  $C_{31}H_{62}O_1$  or  $C_{21}H_{38}O_1$ , corresponding to the ketones expected from an iron carboxylate decomposition reaction (reaction 4). The  $O_1$  DBE vs carbon number plot for the blank, however, exhibits a range of compositions spanning  $\sim C_{20}$ – $C_{50}$  and DBE 1 to  $\sim 10$ , with DBE 4 species as the most abundant. Similar species can also be seen in the low-abundance gray regions in the palmitic acid and CxPA sample plots.

**Ketone Derivatization.** To determine if the unknown peaks in the samples and blanks are ketones/aldehydes or another  $O_1$  functionality (e.g., alcohols, phenols, or furans), we chose a commercially available reagent that selectively derivatizes ketones or aldehydes (Figure 5).<sup>33</sup> Because the

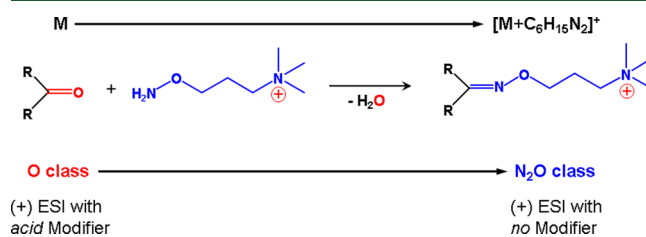


**Figure 5.** Ketone derivatization scheme with Amplifex keto-reagent.

reagent contains a charged quaternary ammonium group, the derivatized samples can be analyzed by (+) ESI without addition of any modifier. The DBE vs carbon number distribution for  $N_2O$  class was processed by subtracting six carbon atoms and two nitrogen atoms (added upon reaction with the reagent) to obtain appropriate compositional representation for the precursor ketones. Figure 6 presents the DBE vs carbon number images for the two samples, upon removal of additional carbons and heteroatoms added from reaction with the derivatization reagent. After derivatization of

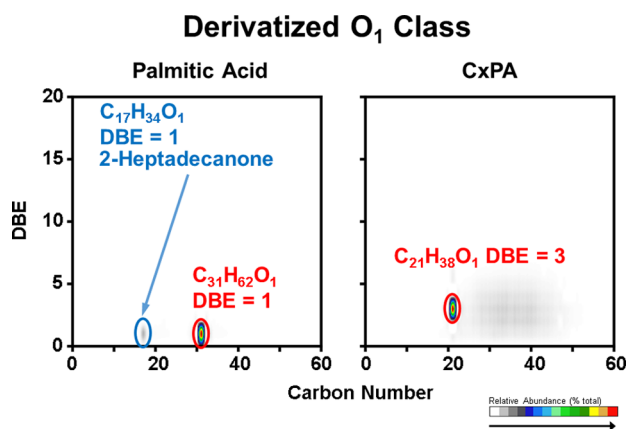


**Figure 6.** DBE versus carbon number plot for members of the  $O_1$  class derivatized with Amplifex keto reagent that targets ketones and aldehydes. The plots have been abridged to remove additional carbon and nitrogen from the reagent, so as to more clearly reveal the reactive molecules. The highly abundant species are identified and confirmed to be acid corrosion products. Additional species can be seen in CxPA sample, at carbon number and DBE similar to those for unknown species seen in Figure 4. Although present at very low relative abundance, their identification confirms that dissolved oxygen contributes to the formation of ketones under the experimental conditions.

the palmitic acid sample, two species are assigned,  $C_{31}H_{62}O_1$  and  $C_{17}H_{34}O_1$  (the molecular formula of 2-heptadecanone). The assignments match those assigned by GC-MS. In the derivatized CxPA sample, the previously detected  $C_{21}H_{38}O_1$  was verified. Because their molecular formulas match those for the expected ketones and what was observed by GC-MS, we conclude that these molecules are ketones rather than aldehydes. No species that contain carbonyls are detected in the derivatized blank sample. Therefore, the  $O_1$  ions with high carbon number and DBE from the underivatized blank are presumably oxidation artifacts of the corrosion test. Further, no higher oxygen species (e.g.,  $O_2$  and  $O_3$  species) reacted with the derivatization reagent, suggesting that the higher  $O_x$  species are not ketones.

**Dissolved Oxygen Interference.** The high carbon number/DBE compositional complexity of  $O_1$  species in the blank suggests that they may arise from oxidized reaction products from the mineral oil. Because the only peaks resolved by GC-MS for the DCM and MeOH fractions of the test samples corresponded to the acid or its ketone, and none were detected in the blank, it is probable that these  $O_1$  species are the primary species in the UCM. No significant corrosion (loss of iron) was measured in the blank corrosion test, suggesting that  $O_1$  formation proceeded by a different mechanism. We suggest that oxidation of the white oil at corrosion test temperature(s) may occur during the corrosion test. Dissolved oxygen is not suspected of being a major driving force behind NAP corrosion and thus is commonly ignored. In the corrosion tests, the headspace was flushed with  $N_2$  but the model acid solutions were not. Based on the diffusivity of oxygen into oil, we estimate that the concentration of dissolved oxygen remains close to air saturation levels for hydrocarbons ( $\sim 70$  ppm).<sup>50</sup> At 316 °C, hydrocarbons can be converted by free radical mechanisms to a variety of oxidized species with various polarities. Although these species may not participate in acid corrosion, they might interfere with isolation and characterization of the ketones. Although they are not a significant

portion of the sample mass (less than 0.1% of the blank mass), in future studies, corrosion test samples should be degassed prior to tests to minimize such interference.

#### 4. CONCLUSIONS

Naphthenic acids react with iron to form iron naphthenates that may thermally decompose into ketones with structures characteristic of the reactive acids, so a method of isolating ketones by SAX chromatography and detection by FT-ICR MS was developed. This method was validated by the study of the corrosion products from separate corrosion tests for two model acids: palmitic and cyclohexane pentanoic acids. Ketones were successfully isolated in a fraction with minimum hydrocarbon and residual acid carryover, confirmed by GC-MS. Direct FT-ICR MS analysis of the ketone fraction reveals the presence of highly abundant ions with molecular formulas that match the ketones expected to be generated by iron carboxylate decomposition; however, additional  $O_1$  species of unknown origin were also detected. Derivatization with a ketone/aldehyde targeting reagent, along with GC-MS fragmentation patterns, confirm that the highly abundant species is a ketone but also reveals that a portion of the background  $O_1$  species is ketones or aldehydes as well. It is believed that those species are generated as a result of dissolved oxygen reacting with hydrocarbons during corrosion test conditions, so future experiments should remove all atmospheric oxygen from the sample before testing. This method will be used in future work to study the acids derived from “real world” petroleum samples and provide a pathway to begin study into the exact mechanism of how the naphthenic acids react with iron.

#### ■ ASSOCIATED CONTENT

##### Supporting Information

The Supporting Information is available free of charge on the ACS Publications website at DOI: 10.1021/acs.energyfuels.7b01803.

Figure S1 caption (PDF)

Total ion chromatogram for the SAX fractions from the CxPA acid sample (Figure S1) (PDF)

#### ■ AUTHOR INFORMATION

##### Corresponding Author

\*Phone: +1 850-644-0529. Fax: +1 850-644-0133. E-mail: marshall@magnet.fsu.edu.

##### ORCID

Peng Jin: 0000-0002-9318-0498

Alan G. Marshall: 0000-0001-9375-2532

Ryan P. Rodgers: 0000-0003-1302-2850

##### Notes

The authors declare no competing financial interest.

#### ■ ACKNOWLEDGMENTS

This work was supported by the National Science Foundation (NSF) Division of Materials Research through DMR-06-54118 and the Institute for Corrosion and Multiphase Technology (ICMT) at Ohio University. The authors also thank Steven M. Rowland for his assistance and helpful discussions regarding the chromatographic separation.

## ■ REFERENCES

- (1) Asrar, N.; MacKay, B.; Birketveit, Ø.; Stopanicev, M.; Jackson, J. E.; Jenkins, A.; Melot, D.; Scheie, J.; Vittonato, J. *Oilf. Rev.* **2016**, *28* (2), 34–49.
- (2) Slavcheva, E.; Shone, B.; Turnbull, A. *Br. Corros. J.* **1999**, *34* (2), 125–131.
- (3) Patrick, B. N.; Chakravarti, R.; Devine, T. M. *Corros. Sci.* **2015**, *94*, 99–103.
- (4) Qu, D. R.; Zheng, Y. G.; Jing, H. M.; Yao, Z. M.; Ke, W. *Corros. Sci.* **2006**, *48* (8), 1960–1985.
- (5) Wu, X. Q.; Jing, H. M.; Zheng, Y. G.; Yao, Z. M.; Ke, W. *Corros. Sci.* **2004**, *46* (4), 1013–1032.
- (6) Babaian-Kibala, E.; Craig, H. L., Jr.; Rusk, G. L.; Blanchard, K. V.; Rose, T.; Uehlein, B. L.; Quinter, R.; Summers, M. A. *Mater. Perform.* **1993**, *32* (4), 50–55.
- (7) Schempp, P.; Preuß, K.; Tröger, M. *Corrosion* **2016**, *72* (6), 843–855.
- (8) Mejia-Miranda, C.; Laverde, D.; Molina V, D. *Energy Fuels* **2015**, *29* (11), 7595–7600.
- (9) Groysman, A.; Brodsky, N.; Penner, J.; Goldis, A.; Savchenko, N. *Mater. Perform.* **2005**, *44*, 34–39.
- (10) Rebak, R. B. *Corros. Rev.* **2011**, 123–133.
- (11) Kane, R. D.; Chambers, B. In *Corrosion Solutions Conference*, Lake Louise, Alberta, Canada, 2011.
- (12) Hau, J. *Corrosion* **2009**, *65*, 831–844.
- (13) Yépez, O. *Fuel* **2005**, *84* (1), 97–104.
- (14) Yépez, O. *Fuel* **2007**, *86* (7–8), 1162–1168.
- (15) Jin, P.; Bota, G.; Robbins, W.; Nescic, S. *Energy Fuels* **2016**, *30* (8), 6853–6862.
- (16) Jin, P.; Robbins, W.; Bota, G. *Corros. Sci.* **2016**, *111*, 822–834.
- (17) Smith, D. F.; Rodgers, R. P.; Rahimi, P.; Teclemariam, A.; Marshall, A. G. *Energy Fuels* **2009**, *23*, 314–319.
- (18) Salih, K. S. M.; Mamone, P.; Dörr, G.; Bauer, T. O.; Brodyanski, A.; Wagner, C.; Kopnarski, M.; Klupp Taylor, R. N.; Demeshko, S.; Meyer, F.; Schünemann, V.; Ernst, S.; Gooßen, L. J.; Thiel, W. R. *Chem. Mater.* **2013**, *25* (8), 1430–1435.
- (19) Chen, C. J.; Chiang, R. K.; Lai, H. Y.; Lin, C. R. *J. Phys. Chem. C* **2010**, *114* (10), 4258–4263.
- (20) Jin, P.; Robbins, W.; Bota, G. *NACE Corrosion* **2016**, 7302.
- (21) Jin, P.; Nescic, S.; Wolf, H. A. *Surf. Interface Anal.* **2015**, *47* (4), 454–465.
- (22) Wolf, H. A.; Cao, F.; Blum, S. C.; Schilowitz, A. M.; Ling, S.; McLaughlin, J. E.; Nescic, S.; Jin, P.; Bota, G. Method for identifying layers providing corrosion protection in crude oil fractions. U.S. Patent 9140640, 2015.
- (23) Barney, M. M.; Miao, T. Z.; Cheng, M. T.; Kusinski, G. J. Methods for evaluating corrosivity of crude oil feedstocks. U.S. Patent 8956874, 2015.
- (24) Rahimi, P.; Kayukawa, T.; Rodgers, R. P.; Teclemariam, A. In *Joint CCQTA/COQA Meeting*, New Orleans, LA, United States.
- (25) Hughey, C. A.; Minardi, C. S.; Galasso-Roth, S. A.; Paspalof, G. B.; Mapolelo, M. M.; Rodgers, R. P.; Marshall, A. G.; Ruderman, D. L. *Rapid Commun. Mass Spectrom.* **2008**, *22*, 3968–3976.
- (26) Hsu, C. S.; Dechert, G. J.; Robbins, W. K.; Fukuda, E. K. *Energy Fuels* **2000**, *14* (1), 217–223.
- (27) Bennett, J. A.; Parlett, C. M. A.; Isaacs, M. A.; Durndell, L. J.; Olivi, L.; Lee, A. F.; Wilson, K. *ChemCatChem* **2017**, *9* (9), 1648–1654.
- (28) Wang, S.; Iglesia, E. *J. Catal.* **2017**, *345*, 183–206.
- (29) Meredith, W.; Kelland, S. J.; Jones, D. M. *Org. Geochem.* **2000**, *31* (11), 1059–1073.
- (30) Wenger, L. M.; Davis, C. L.; Isaksen, G. H. *SPE Reserv. Eval. Eng.* **2002**, *5* (5), 375–383.
- (31) Saab, J.; Mokbel, I.; Razzouk, A. C.; Ainous, N.; Zydowicz, N.; Jose, J. *Energy Fuels* **2005**, *19* (2), 525–531.
- (32) Mediass, H.; Grande, K. V.; Hustad, B. M.; Rasch, A.; Rueslåtten, H. G.; Vindstad, J. E. In *SPE 5th International Symposium on Oilfield Scale*, Aberdeen, U.K., 2003.
- (33) Alhassan, A.; Andersson, J. T. *Energy Fuels* **2013**, *27* (10), 5770–5778.
- (34) Ruddy, B. M.; Huettel, M.; Kostka, J. E.; Lobodin, V. V.; Bythell, B. J.; McKenna, A. M.; Aeppli, C.; Reddy, C. M.; Nelson, R. K.; Marshall, A. G.; Rodgers, R. P. *Energy Fuels* **2014**, *28* (6), 4043–4050.
- (35) Kaiser, N. K.; Quinn, J. P.; Blakney, G. T.; Hendrickson, C. L.; Marshall, A. G. *J. Am. Soc. Mass Spectrom.* **2011**, *22* (8), 1343–1351.
- (36) Blakney, G. T.; Hendrickson, C. L.; Marshall, A. G. *Int. J. Mass Spectrom.* **2011**, *306* (2–3), 246–252.
- (37) Senko, M. W.; Hendrickson, C. L.; Emmett, M. R.; Shi, S. D.-H.; Marshall, A. G. *J. Am. Soc. Mass Spectrom.* **1997**, *8*, 970–976.
- (38) Kaiser, N. K.; Savory, J. J.; McKenna, A. M.; Quinn, J. P.; Hendrickson, C. L.; Marshall, A. G. *Anal. Chem.* **2011**, *83* (17), 6907–6910.
- (39) Tolmachev, A. V.; Robinson, E. W.; Wu, S.; Kang, H.; Lourette, N. M.; Pasa-Tolic, L.; Smith, R. D. *J. Am. Soc. Mass Spectrom.* **2008**, *19* (4), 586–597.
- (40) Savory, J. J.; Kaiser, N. K.; McKenna, A. M.; Xian, F.; Blakney, G. T.; Rodgers, R. P.; Hendrickson, C. L.; Marshall, A. G. *Anal. Chem.* **2011**, *83* (5), 1732–1736.
- (41) Xian, F.; Hendrickson, C. L.; Blakney, G. T.; Beu, S. C.; Marshall, A. G. *Anal. Chem.* **2010**, *82* (21), 8807–8812.
- (42) Shi, S. D.-H.; Drader, J. J.; Freitas, M. A.; Hendrickson, C. L.; Marshall, A. G. *Int. J. Mass Spectrom.* **2000**, *195/196*, 591–598.
- (43) Ledford, E. B.; Rempel, D. L.; Gross, M. L. *Anal. Chem.* **1984**, *56* (14), 2744–2748.
- (44) Hughey, C. A.; Hendrickson, C. L.; Rodgers, R. P.; Marshall, A. G.; Qian, K. *Anal. Chem.* **2001**, *73*, 4676–4681.
- (45) Corilo, Y. E. Florida State University.
- (46) Smith, D. F.; Rahimi, P.; Teclemariam, A.; Rodgers, R. P.; Marshall, A. G. *Energy Fuels* **2008**, *22*, 3118–3125.
- (47) Qian, K.; Robbins, W. K.; Hughey, C. A.; Cooper, H. J.; Rodgers, R. P.; Marshall, A. G. *Energy Fuels* **2001**, *15* (6), 1505–1511.
- (48) Alper Aydin, A. *Sol. Energy Mater. Sol. Cells* **2013**, *113*, 44–51.
- (49) Aydin, A. A.; Aydin, A. *Sol. Energy Mater. Sol. Cells* **2012**, *96* (1), 93–100.
- (50) Ju, L. K.; Ho, C. S. *Biotechnol. Bioeng.* **1989**, *34* (9), 1221–1224.